Proc. Natl. Acad. Sci. USA
Vol. 88, pp. 10586–10590, December 1991
Biochemistry

Immunoglobulin-like PapD chaperone caps and uncaps interactive surfaces of nascently translocated pilus subunits

(biogenesis/pathogenesis/adhesive pili/periplasmic transport)

META J. KUEHN, STAFFAN NORMARK, AND SCOTT J. HULTGREN*

Department of Molecular Microbiology, Box 8230, Washington University School of Medicine, St. Louis, MO 63110

Communicated by Carl Frieden, August 21, 1991

ABSTRACT **Molecular chaperones are found in the cytoplasm of bacteria and in various cellular compartments in eukaryotes to maintain proteins in nonnative conformations that permit their secretion across membranes or assembly into oligomeric structures. Virtually nothing, however, has been reported about a similar requirement for molecular chaperones in the periplasm of Gram-negative bacteria. We used the well-characterized P pilus biogenesis system in *Escherichia coli* as a model to elucidate the mechanism of action of a periplasmic chaperone, PapD, which is specifically required for P pilus biogenesis. PapD probably associates with at least six P pilus subunits after their secretion across the cytoplasmic membrane, but PapD is not incorporated into the pilus. We used purified periplasmic complex that PapD forms with the PapG adhesin to investigate the function of interactions between the chaperone and its targets. We demonstrated that PapD binds to PapG to form a stable, discrete bimolecular complex and that, unlike cytoplasmic chaperones, the periplasmic PapD chaperone maintained PapG in a native-like conformation. Bound PapD in the complex was displaced by free PapD *in vitro*; however, the *in vivo* release of subunits to the nascent pilus is probably driven by an ATP-independent mechanism involving the outer membrane protein PapC. In addition, the binding of PapD to PapG *in vitro* prevented aggregation of PapG. We propose that the function of PapD and other periplasmic pilus chaperones is to partition newly translocated pilus subunits into assembly-competent complexes and thereby prevent nonproductive aggregation of the subunits in the periplasm. These data provide important information for understanding the mechanism of action of this general class of chaperones that function in the periplasmic space.**

PapD is a representative member of a large family of pilus chaperones found at least in *Escherichia coli, Haemophilus influenzae*, and *Klebsiella pneumoniae*. Based on sequence information and the crystal structure of PapD, members of this family have similar structures consistent with the overall topology of an immunoglobulin fold (A. Holmgren, M.J.K., C.-I. Branden, S.J.H., unpublished data). PapD is a specific molecular chaperone that modulates the assembly of protein protomers into P pili but is not a component of the final structure (1–3). P pili, encoded by the *pap* operon, are composite fibers consisting of flexible adhesive fibrillae joined end-to-end to the pilus rod (M.J.K., J. Heuser, S.N., and S.J.H., unpublished data) on uropathogenic *E. coli* (4–6). The specialized fibrillar structures at the tips of P pili are composed of PapE, PapF, and the α-D-galactopyranosyl-(1-4)-β-D-galactopyranose or Galα(1-4)Gal- (galabiose) binding adhesin PapG (2, 7, 8). The stalk of the pilus is composed of repeating PapA monomers probably arranged in a right-hand helix (9–11). PapH, located at the base of the pilus, is a necessary component of the pilus anchor (12). All of the genes encoding these pilus protein subunits have been sequenced and well characterized (1, 3, 12–15). PapD binds to pilus subunit proteins after they are imported into the periplasmic space (1–3), and stable PapD–PapG and PapD–PapE periplasmic preassembly complexes have been purified (1, 2). These stable preassembly complexes are transported to an assembly site thought to be composed, in part, by the outer membrane protein PapC (16), where the complexes are dissociated and the pilus subunits are polymerized.

The mechanism by which the periplasmic PapD chaperone ensures correct interactions of six different types of pilus subunit proteins so that they are assembled into well-defined composite fibers that have distinct adhesive tip structures is virtually unknown. We used purified PapD–PapG in a series of *in vitro* experiments to investigate the role of PapD in forming these associations and to gain insight into the mechanism of PapD action. The results argue that the role of this protein is to bind to interactive assembly surfaces on its pilus protein targets to prevent nonproductive aggregation of pilus subunits imported into the periplasm. Unlike the cytoplasmic chaperones described to date, substrate proteins bound to the periplasmic chaperone PapD seemed to be maintained in a native-like state. The assembly of pili seems to involve the targeting of chaperone-pilus protein complexes to outer membrane assembly sites, where PapD is dissociated by an unknown ATP-independent mechanism and the released interactive subunit is assembled into the pilus.

MATERIALS AND METHODS

Purification and Characterization of the PapD–PapG Complex. The purification of the PapD–PapG preassembly complex was done by a modification of the described Gal(α1–4)Gal-Sepharose affinity-chromatography method (1) using periplasm from *E. coli* strain C600/pPAP58. PapG was eluted from the affinity column with 10 mM 2-(trimethylsilyl)ethyl-4-*O*-α-D-galactopyranosyl β-D-galactopyranoside [a (trimethylsilyl)ethyl (TMSET) glycoside]. Stability of the PapD–PapG complex in urea was determined by incubating 0.1 μg of the complex in 0–6 M urea for 5 min at 25°C. The preparations were applied to isoelectric focusing (IEF) pI 3–9 gels (Pharmacia) and native PAGE (8–25%, Pharmacia) and analyzed for the presence or absence of native PapD–PapG complex by Coomassie blue staining, silver staining, or immunoblotting with anti-PapD–PapG antiserum.

Amino Acid Analysis and CD Spectroscopy. For amino acid analysis, 0.4 ng of PapD–PapG complex was further purified by HPLC on a gel-filtration Spherogel TSK 3000SW column (Beckman). Ratios of amino acid residues within acid-hydrolyzed PapD–PapG complex were compared with the numbers of amino acids in PapD and PapG calculated from

The publication costs of this article were defrayed in part by page charge payment. This article must therefore be hereby marked "*advertisement*" in accordance with 18 U.S.C. §1734 solely to indicate this fact.

Abbreviations: IEF, isoelectric focusing; BSA, bovine serum albumin.

*To whom reprint requests should be addressed.

translated nucleotide sequences (2, 8). The experimentally determined amino acid ratios of the PapD–PapG complex corresponded to a 1:1 ratio of PapD to PapG. Secondary structure of PapG was deduced from CD spectra (Jasco J-600 spectrophotometer, 190–250 nm) of equal concentrations of PapD in samples of PapD and PapD–PapG complex.

Immunoblot Analysis. Samples were boiled in sample buffer and run on SDS/PAGE. Gels were transferred to poly(lvinylidene difluoride) paper (Millipore) and blocked with 1% bovine serum albumin (BSA) in blocking buffer (0.5% Tween/0.5 M NaCl/10 mM Tris, pH 8.2). The blots were incubated for 1 hr at 25°C with rabbit anti-PapD and anti-PapD–PapG antibodies diluted 1:100 in blocking buffer. After three washes in blocking buffer, the blots were incubated for 1 hr at 25°C with alkaline phosphatase-conjugated anti-rabbit antiserum (Sigma) diluted 1:500 in blocking buffer. After three washes in blocking buffer and in developing buffer (3 mM $MgCl_2$/50 mM Tris, pH 9.8), the blots were developed with 5-bromo-4-chloro-3-indolyl phosphate at 50 μg/ml and 0.01% nitro blue tetrazolium in developing buffer.

Radiolabeling of PapD. PapD was purified as described (2). ^{125}I labeling of PapD was done by incubating 8 μg of PapD with 0.5 mCi (1 Ci = 37 GBq) of ^{125}I and 10 μl of chloramine T (2 mg/ml) in 100 μl of phosphate-buffered saline (120 mM NaCl/2.7 mM KCl/10 mM phosphate buffer salts, pH 7.4; Sigma) for 1 min at 25°C. Twenty-five microliters of sodium bisulfite (2 mg/ml) and 100 μl of NaI (2 mg/ml) were then added. Unincorporated ^{125}I was separated from ^{125}I-labeled PapD by using a PD10 column in phosphate-buffered saline/0.1% BSA. Fractions were collected, and the radioactive peak fractions were pooled.

PapD Exchange Reaction. Two tenths of a microgram of PapD–PapG complex in 1 M NaCl/phosphate-buffered saline, pH 7.4 was incubated with 3 volumes of 0–12 ng of ^{125}I-labeled PapD for 5 min at 25°C and then applied to IEF gels (pI 3–9). The IEF gels were Coomassie blue stained and autoradiographed.

Quantitation of PapD–PapG by Densitometry. Silver-stained IEF gels were scanned by using an LKB Ultroscan XL laser densitometer (Pharmacia) at 633 nm, and the ODs of the bands corresponding to PapD–PapG (pI 7.4) were determined.

PapD–PapG Restoration Assay. Fifty nanograms of PapD–PapG preassembly complex in phosphate-buffered saline (pH 7.4) was incubated with 30 ng of BSA in a final concentration of 10 mM dithiothreitol and 4 M urea for 20 min at 25°C. The complex was then diluted into solutions containing 4–600 ng of purified PapD or BSA in water to final concentrations of 1.3 M urea and 3.3 mM dithiothreitol and incubated for 5 min at 25°C. The preparations were applied to IEF gels (pI 3–9), silver stained, and analyzed by densitometry.

RESULTS

Biochemical Properties of Chaperone–Adhesin Complex. The PapD–PapG preassembly complex was isolated and purified from the periplasmic space as described (1) based on its ability to bind specifically to Gal(α1-4)Gal-coated Sepharose. Native PAGE demonstrated that the purified preparation migrated as a discrete bimolecular complex (Fig. 1*A*, lane 1). SDS/PAGE and immunoblotting of the band excised from native gels suggested that the complex consisted of an equimolar ratio of PapD (28.5 kDa) and PapG (35 kDa) (Fig. 1*A*, lanes 2–4). In addition, the complex was hydrolyzed, and its amino acid composition was determined. The amino acid composition of PapD and PapG deduced from the genetic sequence (2, 8) together with the amino acid analysis confirmed that the preassembly complex consisted of an equimolar ratio of PapD and PapG (data not shown).

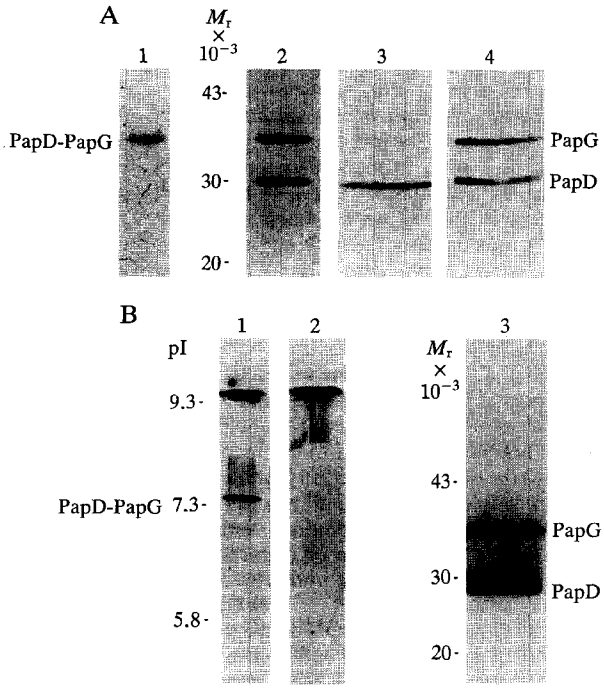

FIG. 1. (*A*) Analysis of the preassembly PapD–PapG complex by PAGE and immunoblotting. Five-tenths microgram of affinity-purified PapD–PapG was analyzed after 8–25% gradient native-PAGE (Pharmacia) (lane 1) and SDS/10–15% PAGE (lane 2) by Coomassie blue staining. The band in lane 1 of the native gel was excised, boiled in SDS sample buffer, and applied to SDS/PAGE for lanes 3 and 4; the gel was immunoblotted with anti-PapD (lane 3) and anti-PapD–PapG antiserum (lane 4). PapD binds to PapG in equimolar amounts to form a discrete bimolecular complex. (*B*) IEF (pI 3–9) gel analysis of the PapD–PapG complex and free PapD. The PapD–PapG complex migrated to a pI of 7.4 (lane 1), whereas PapD alone migrated to a pI of 9.4 (lane 2), as detected by silver staining. The band at pI 7.4 shown in lane 1 was boiled in SDS sample buffer, applied to SDS/PAGE and then immunoblotted by using anti-PapD–PapG antiserum (lane 3). This result confirmed that the polypeptide moiety at pI 7.4 consisted of homogeneous PapD–PapG complexes. pI and molecular weight standards are indicated.

The isoelectric point (pI) of the PapD–PapG complex was determined by IEF to be 7.4 (Fig. 1*B*, lane 1), which is intermediate between the pIs of PapD (pI 9.4) (Fig. 1*B*, lane 2) and PapG (pI 5.1) (17). The composition of the band at pI 7.4 was confirmed to be the PapD–PapG complex by excising the band and analyzing it by SDS/PAGE and immunoblotting (Fig. 1*B*, lane 3). The opposite charge of these proteins at a neutral pH suggests that the binding of PapD to PapG may, in part, involve ionic bonds.

Conformation of Chaperone-Bound Adhesin. Various galabiose analogues have been synthesized and used to compare the receptor-binding chemistry of PapG present at the tips of P pili with PapD-bound PapG isolated from the periplasm (1, 18). Galabiose analogues inhibited hemagglutination mediated by P-piliated bacteria to approximately the same extent that they eluted PapD-bound PapG from Gal(α1-4)Gal-Sepharose (1, 18). In this study, a (trimethylsilyl)ethyl glycoside of galabiose that had a hemagglutination inhibitory power of $\Delta\Delta G = -3.2$ kJ·mol^{-1} ($\Delta\Delta G < 0$ signifies a more potent inhibitor than galabiose) also eluted the PapD–PapG complex efficiently from galabiose Sepharose. Thus, the receptor-binding specificity of periplasmic PapG bound to the chaperone seemed virtually identical to that of PapG incorporated into the tips of pili. The receptor-binding specificity of the adhesin is probably a function of its tertiary structure,

arguing that PapG exists in a native-like conformation within the chaperone complex. Supporting this hypothesis were CD spectra, indicating typical β-pleated sheet structure of PapG within the complex (data not shown).

PapG contains four cysteine residues, as deduced from the genetic sequence. The involvement of these cysteine residues in disulfide bridge formation would most likely affect the mobility of PapG in SDS/PAGE in the presence or absence of 2-mercaptoethanol, as has been reported (19, 20). Under nonreducing conditions, PapG migrated to a lower position than the reduced molecule (Fig. 2). The difference in migration argues that disulfide bonds are present in PapG that is bound to PapD. In summary, these data strongly indicate that unlike other chaperone–substrate complexes, PapG is in a highly folded native-like state within the chaperone complex.

Association Between Chaperone and Adhesin. The dissociation of preassembly chaperone complexes during pilus biogenesis probably is coupled to the incorporation of Pap subunits into the pilus (3). We found that the PapD–PapG complex was very stable, however, and resistant to dissociation in 6 M urea under nonreducing conditions (data not shown). We also tested the ability of PapD to be released from the complex *in vitro* by incubating excess unlabeled PapD–PapG with increased concentrations of ^{125}I-labeled PapD. Increased amounts of radiolabeled PapD–PapG complex (Fig. 3, lanes 1–4) indicated that bound PapD in the PapD–PapG complex was displaced by free ^{125}I-labeled PapD. An alternative explanation of this data, that ^{125}I-labeled PapD simply bound to the PapD–PapG complex, was ruled out because the pIs of labeled and unlabeled complexes were identical. Specificity of the exchange reaction was shown by successfully blocking it with excess unlabeled PapD (Fig. 3, lane 5). Efficient release of the chaperone *in vivo* probably occurs via a mechanism that involves the outer membrane assembly protein PapC.

Role of Chaperone in Capping Interactive Surfaces. Dissociation of the PapD–PapG complex was examined by measuring the intensity of the PapD–PapG band on IEF gels as a function of urea concentration in the presence of 15 mM dithiothreitol. In 2 M urea under reducing conditions, 80% of the complex was destroyed (Fig. 4*A*). In an attempt to restore the native complex from the reduced, denatured preparation, the sample was diluted to conditions in which the complex

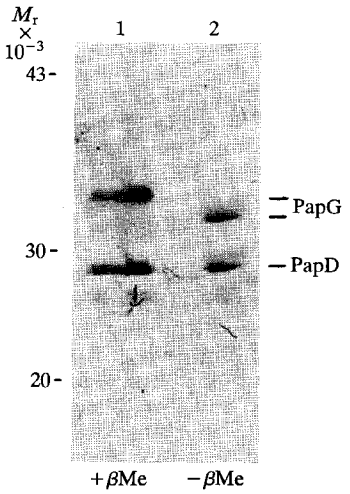

FIG. 2. Identification of disulfide bridges in PapG. PapD–PapG complex was boiled 5 min in SDS sample buffer containing either 5% 2-mercaptoethanol (+βMe) (lane 1) or no reducing agent (−βMe) (lane 2) and analyzed by SDS/PAGE stained with Coomassie blue. The change in PapG migration indicated that disulfide bridges occur in PapG while it is complexed with PapD. Molecular weight standards are indicated.

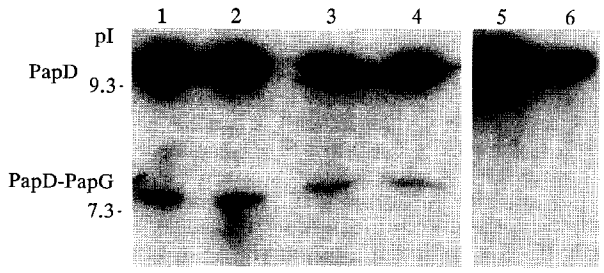

FIG. 3. Displacement of PapD from the PapD–PapG complex. ^{125}I-labeled PapD displaced bound PapD in the PapD–PapG complex as shown by the presence of a radiolabeled IEF band corresponding to ^{125}I-labeled PapD–PapG complex. Note that ^{125}I-labeled PapD–PapG migrated to the same position (pI 7.4) as unlabeled PapD–PapG. Lanes: 1–4, 200 ng of unlabeled PapD–PapG complex incubated with 11, 10, 9, and 8 ng of ^{125}I-labeled PapD, respectively; 5, 100 ng of PapD–PapG complex incubated with a 50-fold excess of unlabeled PapD (200 ng) before 4 ng of ^{125}I-labeled PapD was added; 6, 4 ng of ^{125}I-labeled PapD alone. Preparations were applied to IEF gels and developed by autoradiography. pI standards are indicated.

was previously shown to be stable. IEF analysis of this preparation revealed that the complex did not reform; instead the proteins formed aggregates that were unable to enter the gel (Fig. 4*B*, lane 2). One possible explanation for this result is that the site recognized by PapD is part of a polymerization surface on PapG that interacts with other protein subunits during pilus assembly. The reducing and denaturing conditions may essentially "uncap" this interactive surface, causing aggregation upon removal of denaturant.

Aggregation of subunits in the periplasm is biologically nonproductive. The ability of purified PapD to bind to an interactive surface of PapG and maintain it in a soluble, distinct complex was investigated using an *in vitro* assay modified from Goloubinoff *et al.* (21). A denatured PapD–PapG preparation was diluted and incubated in the presence of increased concentrations of purified PapD. IEF analysis revealed that the amount of restored PapD–PapG complex was proportional to the amount of PapD in the renaturing solution (Fig. 4*C*). In the absence of PapD, aggregation of the proteins prevented reformation of the complex. However, native PapD present in the diluent bound to PapG restored the native soluble complex and thereby prevented aggregation of PapG (Fig. 4*B* and *C*).

DISCUSSION

Pilus chaperones such as PapD are required for pilus formation *in vivo* but reconstitution studies of depolymerized pili *in vitro* have shown that pilus subunits can self-assemble into pili that are morphologically similar to wild-type pili (22, 23). *In vitro* studies using purified PapD–PapG adhesin complex as a prototype have resolved this paradox by showing that the periplasmic PapD chaperone is probably required to prevent premature nonproductive collisions of interactive subunits. PapD consists of two globular domains oriented toward one another in a way that gives the molecule an overall shape of a boomerang. Interestingly, the two domains of PapD have the structural framework similar to an immunoglobulin-variable domain and the human immunodeficiency virus receptor CD4 domain (ref. 24, unpublished data). The cleft of PapD is thought to form part of a binding site important in recognizing a family of related proteins: PapA, PapE, PapF, PapG, PapK, and PapH (1, 24). It seems that PapD binds to newly translocated pilus subunits to partition them into stable, assembly-competent periplasmic complexes that are then targeted to outer membrane sites where the chaperone is dissociated and the pilus subunits are assembled.

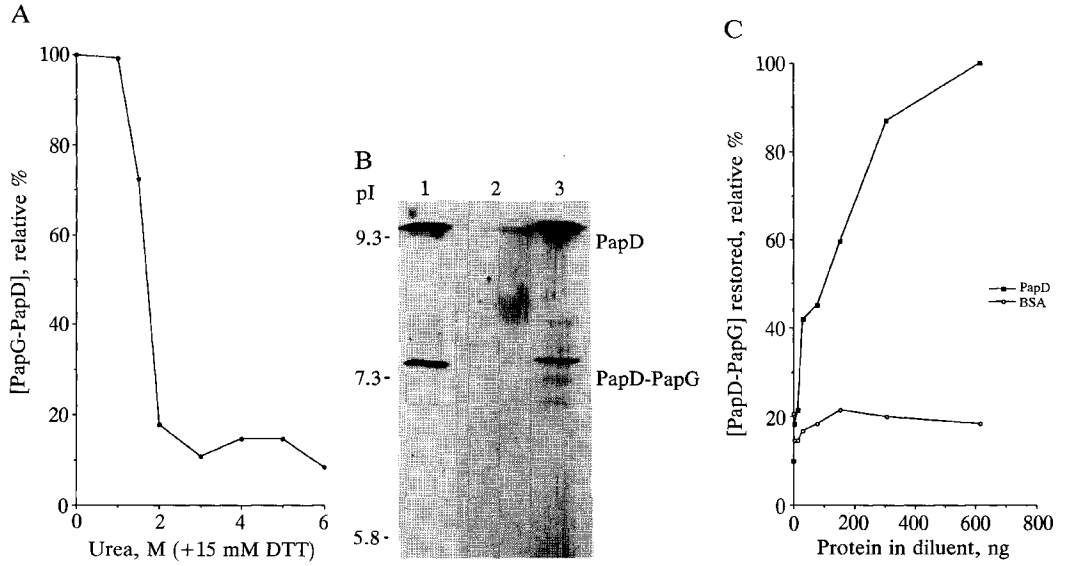

FIG. 4. (*A*) Dissociation of the PapD–PapG preassembly complex. Two-tenths microgram of PapD–PapG was incubated in final concentrations of 0–6 M urea in 15 mM dithiothreitol (DTT) and then loaded onto an IEF gel and silver stained. The gel was scanned by densitometry, and the OD of the band corresponding to PapD–PapG was determined. Relative percentage [PapD–PapG] remaining was calculated by equating the OD of the PapD–PapG band in 0 M urea to 100%. Results indicate that 80% of the complex is destroyed in 2 M urea under reducing conditions. (*B*) PapD prevents aggregation of PapG. Samples were analyzed on an IEF gel after the following treatments: Lanes: 1, 0.8 μg of PapD–PapG complex in water; 2, 0.8 μg of PapD–PapG complex was reduced and partially unfolded in 4 M urea/10 mM dithiothreitol for 20 min at 25°C and then diluted in water to a final concentration of 1.3 M urea/3.3 M dithiothreitol (note that aggregated proteins could not enter gel); 3, restoration of complex was demonstrated when the denatured PapD–PapG preparation was diluted in the presence of 5 μg of PapD to a final concentration of 1.3 M urea/3.3 mM dithiothreitol. pI standards are indicated. (*C*) PapD–PapG restoration assay. Two-tenths microgram of PapD–PapG complex was reduced and denatured in the presence of BSA in a final concentration of 4 M urea/10 mM dithiothreitol. This preparation was then diluted into solutions containing 4–600 ng of purified PapD or BSA in water to final concentrations of 1.3 M urea/3.3 mM dithiothreitol. Products were analyzed on IEF gels and visualized by silver staining. Bands corresponding to PapD–PapG complex were scanned by densitometry and averaged for two separate experiments. Relative percent (PapD–PapG) restored was determined by equating density of the greatest amount of PapD–PapG restored to 100%. The band corresponding to untreated PapD–PapG diluted with an equivalent volume had a relative density of 90–100%. Data indicate that increased amounts of PapD in the diluent resulted in a corresponding increase in restored PapD–PapG complex. Diluent containing BSA was used as a control in this assay and corresponded to a low degree of stabilization of PapD–PapG complex.

Cytoplasmic chaperones such as SecB, trigger factor, and GroEL have been shown to bind nonspecifically to hydrophobic sites on nonnative polypeptides (25–27). In contrast, PapG seems to maintain virtually its same receptor binding specificity whether it is bound to PapD or incorporated into the tip of the pilus. PapG present at the pilus tip and PapG bound to PapD in the PapD–PapG complex seem to bind to the same polar edge of galabiose via hydrogen bonding to hydroxyl groups HO-6,-2′,-3′,-4′, and -6′ (1, 18). Because the binding specificity of PapG is likely to be a function of its tertiary structure, as is the case for most lectins (28–30), these data indicate that PapG exists in a native-like state within the chaperone complex. In addition, it has been shown that when GroEL chaperone was bound to a protein such as dihydrofolate reductase, the bound dihydrofolate reductase was maintained in a nonnative and nonactive state (31). Thus, in contrast to cytoplasmic chaperones, the role of the periplasmic PapD chaperone may be to maintain the bound pilus proteins in native-like states.

Pilus assembly depends on the ability of the chaperone to bind to its targets in a reversible manner. However, the PapD–PapG complex was found stable in 6 M urea under nonreducing conditions, suggesting a strong association between these two proteins. In our *in vitro* experiments, radiolabeled PapD was incorporated into the complex in proportion to the amount of radiolabeled free PapD available, indicating that PapG released PapD and then could bind to free radiolabeled PapD, reforming the complex. *In vivo*, the release of PapD from the preassembly complexes probably occurs via a mechanism that involves the outer membrane protein PapC (16) (Fig. 5). Interaction with PapC may drive the transfer of pilus proteins from preassembly complexes to the growing pilus. PapD does not contain a typical ATP binding domain, such as that found in adenyl kinase (24, 33). Therefore, unlike most cytoplasmic and eukaryotic molecular chaperones (34), ATP is probably not required for dissociation of these complexes. Other pilus proteins correctly oriented in the assembly site probably favor the exchange of a pilus protein associated with PapD to association with another pilus protein already incorporated into the pilus. This reaction may be driven, in part, by a conformational change of the pilus protein, possibly involving the internalization of the PapD-binding site.

Specific sequence homologies among pilus proteins in the amino and carboxyl terminii (13) suggest that PapD may recognize a common epitope on each of the pilus subunit proteins (1). Whether PapD binds native or nonnative epitopes is not yet known. In our model, the surface on the pilus protein recognized by PapD may also form part of the surface that interacts with nascently incorporated subunits in the growing pilus. Thus, PapD may function as a reversible capping protein that modulates polymerization. When PapD is bound to the subunits, aggregation is prevented, whereas its release results in polymerization of the pilus rod. The binding and release of PapD is apparently orchestrated to occur at distinct sites within the cell, guiding the protein protomers along biologically productive pathways. The transport and targeting of chaperone complexes to the outer membrane assembly site occurs by an unknown mechanism but would seem to involve the recognition of the pilus protein protomer in the context of PapD.

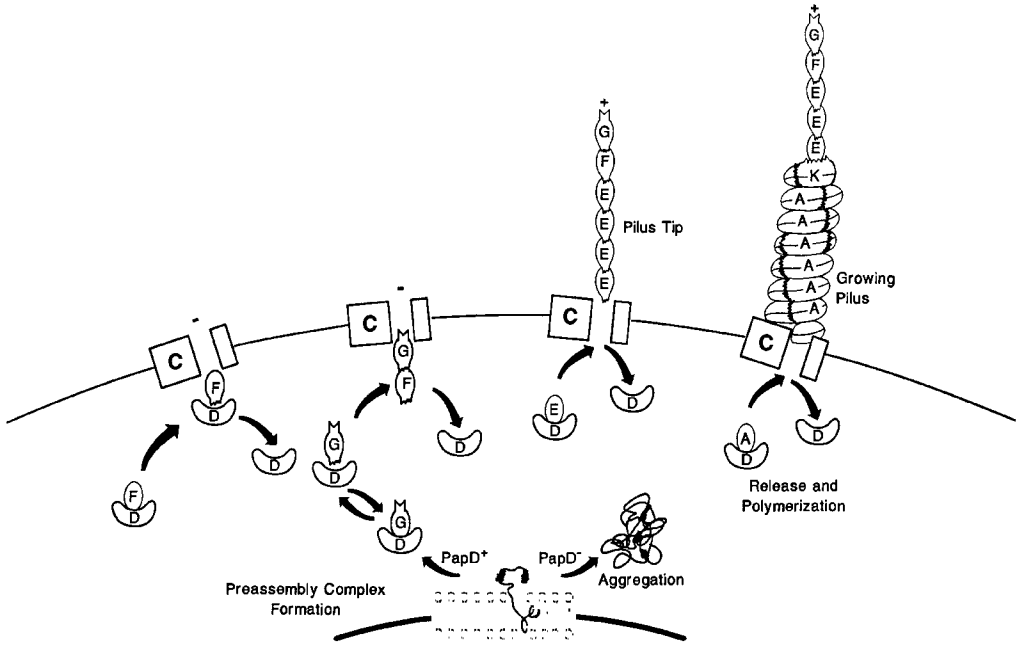

FIG. 5. Model of PapD-assisted pili biogenesis. Four successive stages of assembly are shown from left to right. Letters represent Pap protein subunits. PapE, PapF, PapK, PapA, and PapH probably interact with PapD in the same manner that PapG interacts with PapD in the periplasm. Once PapG is polymerized into tips containing PapF and PapE, the organism is hemagglutination positive (+) (1). The pilus is thought to grow from the base as has been shown for the closely related type 1 pilus (32). The pilus stalk is probably composed of 3 1/8 subunits of PapA per turn of the helix (11). Pilus tips are distinct fibrillar structures as determined by high resolution electron microscopy (M.J.K., J. Heuser, S.N., and S.J.H., unpublished data). The role of PapH (12) to anchor pili to the bacterial cell is not shown. See text for discussion of this model.

We thank Ingela Nilsson and Jerome Pinkner for their expert technical assistance and Soman Abraham for helpful discussions. We also thank Carl Branden for insightful advice and Goran Magnusson for generously supplying synthesized galabiose receptor analogues. This work was supported by grants from Lucille P. Markey Charitable Trust Contract, Washington University/Monsanto Company Biomedical Research Contract, National Institutes of Health Research Grant 1R01AI29549, Institutional Biomedical Research Support Grant 2-S07-RR05389, and aided by Grant IN-36 from the American Cancer Society.

1. Hultgren, S. J., Lindberg, F., Magnusson, G., Kihlberg, J., Tennent, J. M. & Normark, S. (1989) *Proc. Natl. Acad. Sci. USA* **86,** 4357–4361.
2. Lindberg, F., Tennent, J. M., Hultgren, S. J., Lund, B. & Normark, S. (1989) *J. Bacteriol.* **171,** 6052–6058.
3. Hultgren, S. J., Abraham, S. N. & Normark, S. (1991) *Annu. Rev. Microbiol.* **45,** 383–415.
4. O'Hanley, P., Lark, D., Falkow, S. & Schoolnik, G. (1985) *J. Clin. Invest.* **75,** 347–360.
5. Kallenius, G., Svenson, S. B., Hultberg, H., Molby, R., Helin, I., Cedergren, B. & Winberg, J. (1981) *Lancet* **ii,** 1369–1372.
6. Vaisanen, V., Tallgren, L. G., McKela, P. H., Kallenius, G., Hultberg, H., Elo, J., Siitonen, A., Svanborg-Eden, C., Svenson, S. B. & Korhonen, T. (1981) *Lancet* **ii,** 1366–1369.
7. Lindberg, F., Lund, B., Johansson, L. & Normark, S. (1987) *Nature (London)* **328,** 84–87.
8. Lund, B., Lindberg, F., Marklund, B. I. & Normark, S. (1987) *Proc. Natl. Acad. Sci. USA* **84,** 5898–5902.
9. Lindberg, F., Lund, B. & Normark, S. (1984) *EMBO J.* **3,** 1167–1173.
10. Uhlin, B. E., Norgren, M., Baga, M. & Normark, S. (1985) *Proc. Natl. Acad. Sci. USA* **82,** 1800–1804.
11. Brinton, C. C. (1965) *Trans. N.Y. Acad. Sci.* **27,** 1003–1054.
12. Baga, M., Norgren, M. & Normark, S. (1987) *Cell* **49,** 241–251.
13. Tennent, J. M., Lindberg, F. & Normark, S. (1990) *Mol. Microbiol.* **4,** 747–758.
14. Lindberg, F., Lund, B. & Normark, S. (1986) *Proc. Natl. Acad. Sci. USA* **83,** 1891–1895.
15. Baga, M., Normark, S., Hardy, J., O'Hanley, P., Lark, D., Olsson, O., Schoolnik, G. & Falkow, S. (1984) *J. Bacteriol.* **157,** 330–333.
16. Norgren, M., Baga, M., Tennent, J. M. & Normark, S. (1987) *Mol. Microbiol.* **1,** 169–178.
17. Hoschutzky, H., Lottspeich, F. & Jann, K. (1989) *Infect. Immunol.* **57,** 76–81.
18. Kihlberg, J., Hultgren, S. J., Normark, S. & Magnusson, G. (1989) *J. Am. Chem. Soc.* **111,** 6364–6368.
19. Strom, M. S., Nunn, D. & Lory, S. (1991) *J. Bacteriol.* **173,** 1175–1180.
20. Richardson, N. E., Brown, N. R., Hussey, R. E., Vaid, A., Mathews, T. J., Bolognesi, D. P. & Reinherz, E. L. (1988) *Proc. Natl. Acad. Sci. USA* **85,** 6102–6106.
21. Goloubinoff, P., Christeller, J. T. & Gatenby, A. A. (1989) *Nature (London)* **342,** 884–888.
22. Abraham, S. N., Hasty, D. L., Simpsin, W. A. & Beachey, E. H. (1983) *J. Exp. Med.* **158,** 1128–1144.
23. Eshdat, Y., Silverblatt, F. J. & Sharon, N. (1981) *J. Bacteriol.* **148,** 308–314.
24. Holmgren, A. & Branden, C. I. (1989) *Nature (London)* **342,** 248–256.
25. Hardy, J. S. & Randall, L. L. (1991) *Science* **251,** 439–443.
26. Lecker, S., Lill, R., Ziegelhoffer, T., Georgopoulos, C., Bassford, P. J., Kumamoto, C. A. & Wickner, W. (1989) *EMBO J.* **8,** 2703–2709.
27. Lecker, S. H., Driessen, A. J. M. & Wickner, W. (1990) *EMBO J.* **9,** 2309–2314.
28. Argos, P., Mahoney, W. D., Hermodson, M. A. & Hanei, M. (1981) *J. Biol. Chem.* **256,** 4357–4361.
29. Weis, W., Brown, J. H., Cusack, S., Paulson, J. C., Skehel, J. J. & Wiley, D. C. (1988) *Nature (London)* **333,** 426–431.
30. Vyas, N. K., Vyas, M. N. & Quiocho, F. A. (1988) *Science* **242,** 1290–1295.
31. Martin, J., Langer, T., Boteva, R., Schramel, A., Horwich, A. L. & Hartl, F.-U. (1991) *Nature (London)* **352,** 36–42.
32. Lowe, M. A., Holt, S. C. & Eisenstein, B. I. (1987) *J. Bacteriol.* **169,** 157–163.
33. Schulz, G. E., Elzinga, M., Marx, F. & Schirmer, R. H. (1974) *Nature (London)* **250,** 120–123.
34. Rothman, J. E. (1989) *Cell* **59,** 591–601.